Environ Sci Pollut Res (2016) 23:22027–22036
DOI 10.1007/s11356-016-7439-x

RESEARCH ARTICLE

Catalytic reduction of hexavalent chromium by a novel nitrogen-functionalized magnetic ordered mesoporous carbon doped with Pd nanoparticles

Sisi Li[1,2] · **Lin Tang**[1,2] · **Guangming Zeng**[1,2] · **Jiajia Wang**[1,2] · **Yaocheng Deng**[1,2] · **Jingjing Wang**[1,2] · **Zhihong Xie**[1,2] · **Yaoyu Zhou**[1,2]

Received: 10 May 2016 / Accepted: 8 August 2016 / Published online: 19 August 2016

Abstract Hexavalent chromium Cr(VI) is a toxic water pollutant which can cause serious influence to the health of the human and animals. Therefore, developing new methods to remove hexavalent chromium in water attracts great attention of scholars. In our research, we successfully synthesized a new type of magnetic mesoporous carbon hybrid nitrogen (Fe-NMC) loaded with catalyst Pd nanoparticles (NPs), which performed excellent catalytic reduction efficiency toward Cr(VI). The characterization of Pd/Fe-NMC composite was investigated in detail using scanning electron microscope (SEM), high-resolution transmission electron microscopy (HRTEM), Fourier transform infrared spectroscopy (FTIR), and nitrogen adsorption-desorption measurements. According to the experimental results, we dealt with in-depth discussion and studied on the mechanism of hexavalent chromium removed by Pd/Fe-NMC composite. Furthermore, the batch experiments were conducted to investigate the catalytic reduction ability of composite. It was found that the chromium reduction process conforms to pseudo-first-order reaction kinetics model when the concentrations of chromium and sodium formate were low. It took only 20 min for the Pd/Fe-NMC composite to reach 99.8 % reduction of Cr(VI) (50 mg/L). The results suggested that the Pd/Fe-NMC composite may exhibit significantly improved catalytic activity for the hexavalent chromium reduction at industrial wastewater.

Keywords Pd · Hybrid nitrogen · Magnetic mesoporous carbon · Hexavalent chromium · Catalytic reduction · Wastewater

Responsible editor: Suresh Pillai

✉ Lin Tang
tanglin@hnu.edu.cn

✉ Guangming Zeng
zgming@hnu.edu.cn

[1] College of Environmental Science and Engineering, Hunan University, Changsha 410082, People's Republic of China

[2] Key Laboratory of Environmental Biology and Pollution Control, (Hunan University), Ministry of Education, Changsha 410082, People's Republic of China

Introduction

Hexavalent chromium (Cr(VI)) is commonly used in the process of industrial production such as steel industry (Kim et al. 2002), auto preserving, and clothing making (Donmez and Aksu 2002). However, serious chromium pollution has occurred due to its leaking and improper use in technological production (Pang et al. 2011a). As is known to all, Cr(VI) is regarded as a major toxic pollutant of the world (Krishnani et al. 2013) and has been proved to increase risk of DNA mutation (Tang et al. 2014), which has carcinogenicity and acute toxicity as well (Zhou et al. 1993). By comparison, Cr(III) is relatively nontoxic, inert, and less mobile, even as a well-known nutrient of lipid and sugar metabolism for human and animals compared with Cr(VI) (Elliott and Zhang 2001). Therefore, it has caused great attention to the reduction of Cr(VI) to Cr(III) efficiently in the wastewater and groundwater in scientific society. Recently, to remediate the Cr(VI) pollutant in the groundwater, a few in situ chemical reduction technologies were developed which need addition of reductants into the subsurface, wherein Cr(VI) can be subsequently removed at acidic condition (Mertz 1969; Qian et al. 2014; Chen et al. 2011a). For example, nanosized iron particles have stimulated wide attention on successfully reductive precipitation of Cr(VI) in wastewater purification (Gao and Xia 2011) and groundwater due to their low cost (Jeen et al. 2008). Yet, it

is proposed that chromium ions and Fe oxide formed the precipitate on Fe^0 surface, which hinders the reduction reaction process due to the aggregation (Fruchter 2002). Although redox manipulation that decreases the chromium compound concentrations by the addition of dithionite is demonstrated as an effective method (Basu and Johnson 2012), the amount of reactive irons has always been limited. Consequently, it is of great importance to develop new recovery process which possesses a sustainable capacity to reduce Cr(VI) efficiently.

Nowadays, catalytic reduction supported by palladium (Pd) nanoparticle is proved an outstanding recovery method, and it is illustrated that palladium nanostructures play a significant role in nanomaterial catalysis for the heavy metal removal (Chaplin et al. 2012) and organohalogen contaminant reduction (Yang et al. 2014; Zhou et al. 2016). At the same time, the use of formic acid upon adding Pd particle catalyst to restore Cr(VI) (Chen et al. 2011b) has received increasing investigation on account of its convenience and practicability (Liang et al. 2014). On the one hand, H_2 and CO_2 were produced through formic acid decomposition ($HCOOH \rightarrow CO_2 + H_2$) (Huang et al. 2012). On the other hand, the reduction of Cr(VI) to Cr(III) occurred by H_2 transfer due to the H_2 adsorbed on Pd surface ($Cr_2O_7^{2-} + 8H^+ + 3H_2 \rightarrow 2Cr^{3+} + 7H_2O$) (Hu et al. 2012). However, there is a barrier to research the moderate oxidation ability of Cr(VI) in neutral conditions. The solubility of Cr(III) and the oxidation potential of Cr(VI) observably increase with the decreasing pH of aqueous solution significantly. It is thus nonetheless worth noting a new carrier to fix Pd to make Cr(VI) sedimentation process highly active which can be successfully applied as catalytic reduction method in water treatment. For example, Wei et al. utilized amino-functionalized palladium nanowires to reduce hexavalent chromium effectively (Wei et al. 2015). Also, the palladium nanoparticles for catalytic reduction of Cr(VI) using formic acid were researched by Omole MA's group (Omole et al. 2007).

According to previous research, mesoporous composite materials (Chen et al. 2011b) may be in favor of attaching metal particles for their large surface area and pore volume, as well as high stability under ambient conditions (Shevchenko et al. 2008). What's more, the faster electron-transport mechanism is one of the greatest advantages of mesoporous composites (Ludwig et al. 2007) which brought its abundant employment in wastewater. Besides, it has been reported recently that the loaded metal NPs on mesoporous composite enhanced the catalytic reduction activities of Cr(VI) (Bhowmik et al. 2014).

Based on the above consideration, we proposed a novel method to synthesize the magnetic mesoporous carbon-based hybrid nitrogen composites (Fe-NMC) by co-impregnation process in order to overcome the obstacle of low stability and electronic transmission of the materials. The composite not only owns super magnetism but also possesses excellent ability of immobilization and adsorption of metal particles. And then, palladium particles were attached on the Fe-NMC composites to form a new catalyst (Pd/Fe-NMC). To evaluate the property improvement of the functionalized mesoporous carbon and to provide valuable information for removing water metal contaminants, this material was firstly used for Cr(VI) catalytic reduction with sodium formate as a reducing agent in the wastewater. Also, HCOONa was used as electron donor and to buffer the solution pH in this study. Moreover, the prepared composites were characterized using transmission electron microscopy (TEM), scanning electron microscope (SEM, JEOL JSM-6700), Raman, and Fourier transform infrared spectroscopy (FTIR), and the catalytic reduction mechanism was also analyzed through study of the catalytic reaction parameters and kinetics.

Materials and methods

Synthesis of the Fe/NMC composite

The synthesis of magnetic Fe/NMC composite used SBA-15 (Zhao et al. 1998) as the hard template, while its alloy source and carbon source were metal nitrates and furfuryl amine, respectively (Wang et al. 2010). Firstly, we dissolved 1.082 g metal nitrates into 10-mL ethanol solution and then used the incipient wetness impregnation technique to blend 1 g of SBA-15 into the above mixed solution. After full erosion, 2 mL furfuryl amine was mixed to form multicomponent solution under stirring. Subsequently, the furfuryl amine was thoroughly polymerized in the dipping mesoporous materials in the air for 10 h at 80 °C. Furthermore, the composite was carbonized in N_2 at 900 °C for 2 h with a heating rate of 2 °C min^{-1}, and the poly furfuryl alcohol was also calcined at high temperature which in situ reduced the metal oxides to alloy. After calcination, the composite was washed with heated 2-M NaOH solution to remove residual silicon. The synthetic Fe/NMC was acquired by filtering with a PVDF membrane (0.45 μm), washing with water, and dried at 70 °C.

Fabrication of Pd/Fe-NMC composite

The Pd/Fe-NMC composite was fabricated by a simple ultrasound-assisted method as follows (Jin and Lee 2014). Firstly, 0.05 g $PdCl_2$ was dispersed in 5-mL HCL (1 M) solution at 60 °C in a 25-mL flask by ultrasound. After treatment by ultrasound for 30 min, then pH meter was used to adjust the pH of the solvent to neutral by adding NaOH (1 M) solution. Secondly, 0.5 g Fe/NMC was added into flask and stirred on magnetic stirrer for another 30 min until the compound was fully mixed. A solution of formic acid (10 mL, 3 M) was added in above aqueous solutions by a syringe and was kept in the water bath pot for 4 h. Thirdly, the samples were washed

with deionized water several times and dried in the oven at 60 °C overnight. Finally, the Pd/Fe-NMC composite was obtained. The prepared process is shown in Fig. 1.

Characterization

The transmission electron microscopy (TEM, JEOL JEM-1230) was used to observe the morphology of samples, and the scanning electron microscope (SEM, JEOL JSM-6700) was utilized to characterize the structure and images of composite. The analysis in the SEM image was observed by energy dispersive X-ray (EDX), and Raman spectrometry (LabRam HR800) characterized the electronic states of the surface of the resultant sample. The possible existing functional groups and compositions were investigated by FTIR spectrometer (Nicolet NEXUS 670). And then, we used continuous flow techniques to detect the BET surface areas of all samples which were measured at 77 K by quantachrome instruments for NOVA adsorption analyzer. The zeta potential and magnetization of the samples were detected by some other texting measurements, such as Zetasizer Nano (ZEN3600, Malvern) and vibrating sample magnetometer (VSM National Institute of Metrology, respectively).

Catalytic Cr(VI) reduction experiments

In the research, the batch experiment as the major method of Cr(VI) reduction reaction was used to assess the catalyst activities, with the reaction scheme shown in Fig. 2. It was carried out in 50-mL stoppered conical flasks for realizing catalysis tests containing $K_2Cr_2O_7$ (50 mg/L) and HCOONa (600 mg/L) by shaking at 150 rpm in a water bath shaker at 30 °C. Meanwhile, the pH values of the solutions were adjusted to 2.0 with 0.1 mol L^{-1} H_2SO_4 solution. The reason for adding H_2SO_4 can maintain the acidity of solution and be conducive to atomic H transfer with Cr(VI) ion. Moreover, it is not easy to volatilize under the temperature control test which is powerful for Cr(VI) reduction. Typically, in order to promote the reduction reaction of Cr(VI), we dispersed 8 mg of Pd/Fe-NMC composite catalyst into aqueous solution (10 mL). After finishing every cycle, the Pd/Fe-NMC composite was magnetically separated and dried at 60 °C overnight. Furthermore, the supernatants were collected through fluid filtration approach for residual chromium contaminant concentration measurement. The color agent was used to detect Cr(VI) concentration in the quartz colorimetric utensil by UV-754N spectrophotometer at a fixed wavelength of 540 nm (Wei et al. 2015). The Perkin-Elmer Analyst 700 (AAS, Perkin-Elmer, USA) atomic absorption spectrophotometer was used to determine the final concentrations of Cr(VI) and Cr(III). The conversion was expressed in percentage to represent the extent of the catalytic reduction calculated by Eq. (1).

$$\text{Conversion} = \left(\text{Cr(VI)}_0 - \text{Cr(VI)}\right)/\text{Cr(VI)}_0 \quad (1)$$

where $Cr(VI)_0$ is the initial concentration and Cr(VI) is the concentration at certain time point. The conversion between the $Cr(VI)_0$ and Cr(VI) was taken as the catalyst activity for reducing Cr(VI). In addition, a control experiment was carried out in duplicate to make sure the accuracy of the experiment.

Control and recycle studies

The Pd/Fe-NMC catalysts were tested for the balance of stability and repeatability in recycling for two more catalytic reactions. After accomplishment of the chromium catalytic reduction experiments, the reflective material was magnetically separated and washed with ultrapure water several times in order to remove the residual compounds (Jin and Lee 2014). Specifically, after rinsing thoroughly by ultrapure water to neutrality, the regenerated Pd/Fe-NMC catalysts were weighed and recycled in order to apply for another reduction experiment.

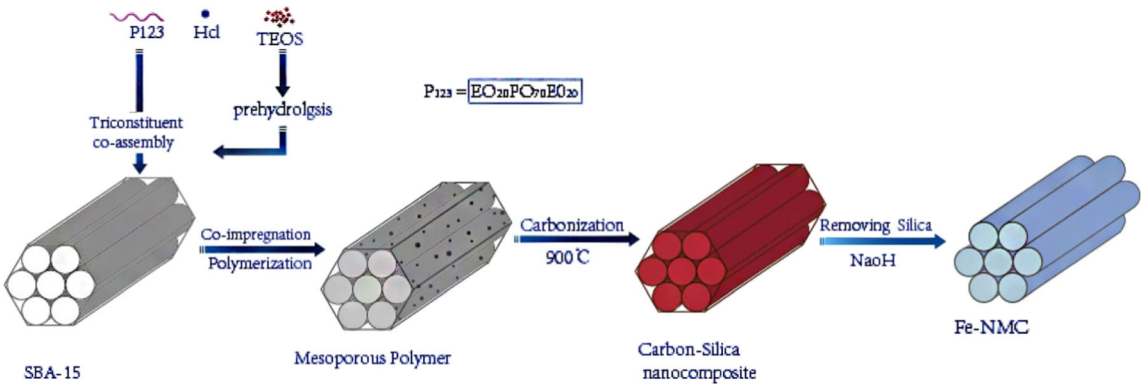

Fig. 1 Synthesis procedure of Fe/NMC

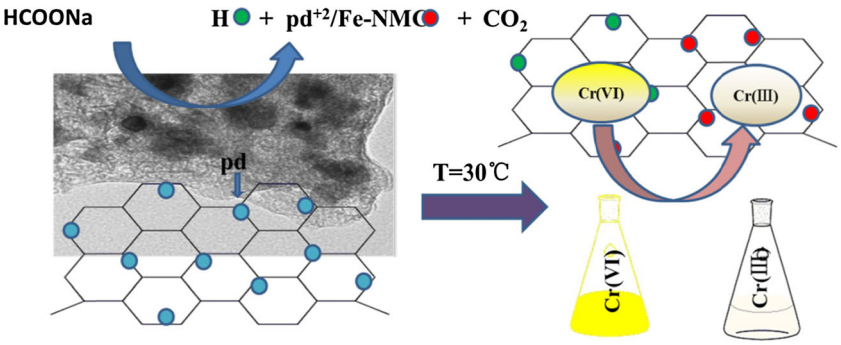

Fig. 2 The proposed reaction scheme of Cr(VI) removed by Pd-Fe/NMC

Results and discussion

Characterization of materials

Figure 3 shows the scanning electron microscope (SEM) and high-resolution transmission electron microscopy (HRTEM) images of the fresh Pd/Fe-NMC and ordered mesoporous carbon (OMC), respectively. The SEM images in Fig.3a, b indicated that the mesoporous carbon composite had rod-like morphology (Liu et al. 2010) and relatively uniform lengths. The HRTEM images (Fig. 3c, d) showed that OMC and Pd/Fe-NMC possessed ordered stripe-like structures and 2D hexagonal pore arrays (Pang et al. 2011b), and the degree of order was clearly observed to decrease to some extent compared with pure OMC, which demonstrated that the ordered mesoporous structure of mesoporous carbon was deteriorated somewhat due to Pd and Fe addition, illustrating further that Fe and Pd precursor was decomposed and reacted with carbon at high temperatures. Pd/Fe-NMC composite could be observed implanted in the carbon clubs (Fig. 3d).

The isotherm curve (Fig. 4) of Pd/Fe-NMC composite showed type IV standard isotherms with a well-defined step in the adsorption curve, around a 0.5–0.7 value of P/Po, indicating that the structure of it contains uniform mesopores. The corresponding pore size distribution confirms that (Fig. 4, inset) the pore size distribution of the carbons centered at near 4.3 nm, which was not found in the previous study (Shrestha et al. 2013). It shows a distinct decrease of BET surface area from 886.3 to 523.5 $m^2\ g^{-1}$ and pore volume from 0.76 to 0.68 $cm^3\ g^{-1}$ due to the introduction of nanoparticles (Table 1). It might be caused by nanoparticles entering into channels occupying partial space of pores, and even blocking mesopores, and the reduction of iron oxide during the decomposition of $Fe(NO_3)_3$ caused the loss of carbon atoms. It is

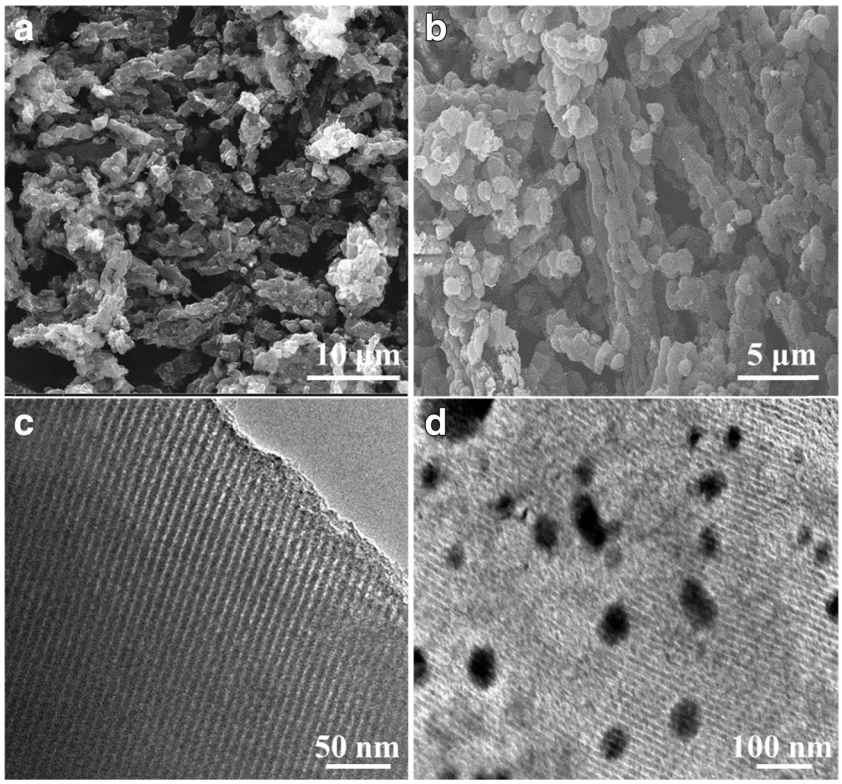

Fig. 3 SEM images of OMC (**a**) and of Pd/Fe-NMC (**b**), and HRTEM images of OMC (**c**) and of Pd/Fe-NMC (**d**)

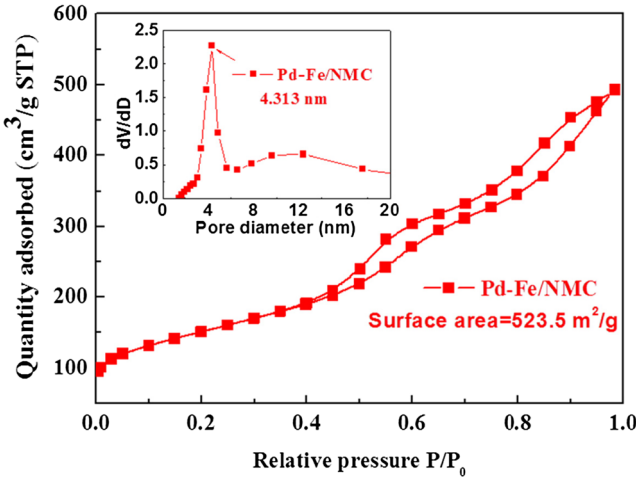

Fig. 4 Nitrogen adsorption–desorption isotherms. Pore size distribution of Pd/Fe-NMC (*inset*)

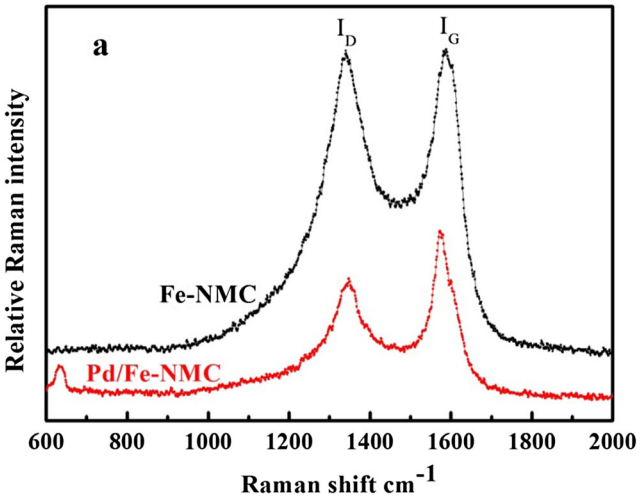

Fig. 5 Raman shift of Pd/Fe-NMC and Fe-NMC

indicated that the Fe-NMC and Pd/Fe-NMC composite both possess a unique structure of D and G mode peaks from Raman spectra (Fig. 5). D patterns located at 1343 cm^{-1} represent the disordered sp^3 hybridization of carbon atoms due to graphite, and G model located at 1583 cm^{-1} is usually associated with E_{2g} vibrational mode of sp^2 hybrid structure of ordered mesoporous carbon atoms (Tang et al. 2014). The ratio between them (I_D/I_G) is a measure of the degree of orderliness and graphitization. It is conducted that the I_D/I_G ratio of Pd/Fe-NMC (1.14) is lower than the ratio of Fe/NMC (1.18) which was estimated from the Raman spectra, showing that the overall graphitization degree of Pd/Fe-NMC is attributed to the introduction of transition metal Pd. As shown in Fig. 6, the functional groups of two nanoparticles were assessed by FTIR spectrometer (Fig. 6). The broad signal centered at around 3000 cm^{-1} possibly corresponds to C-H combined with N-H stretching vibration for Fe-NMC and Pd/Fe-NMC. The band at 1640 cm^{-1} corresponds to the O-H deformation of water or C = O stretching vibration observed in Fe/NMC. The peaks located at 1630 cm^{-1} can be assigned to N-H vibration coupled with C-N stretching mode for Pd/Fe-NMC. The shift between the broad band of Fe-NMC and Pd/Fe-NMC can result from Pd loaded. The common peak for two composites at 1120 cm^{-1} fits in C-O the stretching vibration (Chi et al. 2012), representing the skeleton structure of the mesoporous carbon. Furthermore, the peaks located at 570 cm^{-1} typically fit in Fe-O bond vibration, suggesting that the two materials had magnetic properties (Wang and Lo 2009).

Table 1 Textural properties of the mesoporous carbon composites

Samples	S_{BET} ($m^2\ g^{-1}$)	V_t[a] ($m^3\ g^{-1}$)	D_{BJH}[b] (nm)
OMC	955	0.806	0.632
Fe-NMC	886	0.761	0.513
Pd/Fe-NMC	553	0.683	0.413

BET Brunauer–Emmett–Teller

[a] Total pore volume (P/P_0 = 0.985)

[b] BJH average pore width

Effect of solution pH

Reduction of Cr(VI) by formate was investigated in solutions at different pH values. Initial concentrations of $K_2Cr_2O_7$ (50 mg/L) and HCOONa (600 mg/L) were kept constant. The initial solution pH was adjusted with droplet addition of H_2SO_4 or NaOH through pH meter in conical flasks in the range from 2 to 7. Then, Pd-Fe/NMC (8 mg) was added to promote the catalytical reaction. It indicated that decreasing pH expectedly increased the reducibility of Cr(VI). The ionic equations of redox reaction could be expressed as Eq. (2)–(3) (Fathi 2012).

$$Cr_2O_7^{2-} + 14H_3O^+ + 6e^- \rightarrow Cr^{3+} + 21H_2O; E0(V) = +1.33 \quad (2)$$

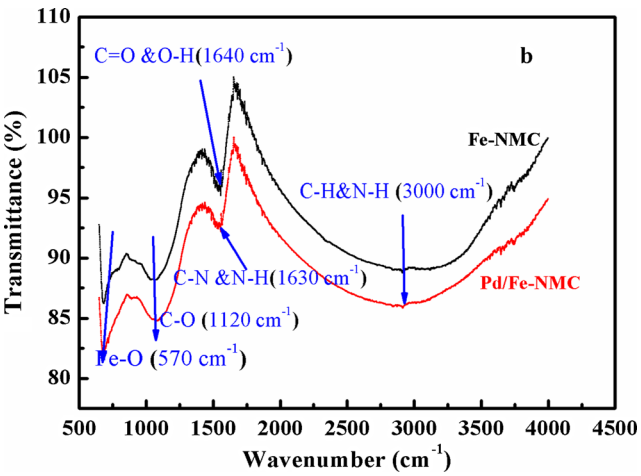

Fig. 6 FTIR spectra of Pd/Fe-NMC and Fe-NMC

$$HCOO^- + H_2O \rightarrow CO_2 + H_3O^+ + 2e^- \quad (3)$$

Figure 7 shows that the removal rates of chromium correspondingly reached 99.97, 99.89, 99.68, and 99.33 % within 20-min period at pH 2.0, 3.0, 5.0, and 7.0, respectively. It is suggested that the acidic environment clearly facilitated the reaction when the reduction rate of Cr(VI) decreased with the increase of pH significantly from 2.0 to 7.0. As can be seen from the experimental data, the optimum reduction pH occurs at about 2.0. Results indicated that low pH was advantageous to the adsorption and decomposition of the reactants formate and dichromate. On one hand, the added droplets of dilute H_2SO_4 can maintain the acidity and be conducive to atomic H transfer. On the other hand, low pH was favorable for the reactants formate and dichromate which are both negatively charged to be adsorbed to the catalyst composites. Also, the kinetics reaction constant matched with previous reports well (Yang et al. 2010). What is more, the pH of the batch experiments remained constant in the whole process in the four cases studied, suggesting that the concentration of the reactant Cr(VI) limited electronic transmission. It is important that the first-order batch kinetics retain consistent in all pH conditions which precisely illuminated that Pd mesoporous catalysts maintained good catalytic reduction activity and physical chemical stability (Wattsa et al. 2015).

Notably, due to the protonation effect of catalyst agents and a strong binding force existing between the ions, it is found that the surface acidities of catalysts increase with pH decreasing at low pH (Ludwig et al. 2007). As a consequence, higher catalytic activities were promoted at lower pH and the catalytic reduction process of Cr(VI) was highly pH dependent.

Effect of temperature

The temperature has a profound effect on Cr(VI) reduction reaction (Fig. 8). To obtain the optimum temperature, various ambient temperatures were tested from 15 to 40 °C at intervals of 5 °C. The initial Cr(VI) removal rate reached 99.97 % in 20 min at 30 °C, which suggested the optimal reaction condition for reducing Cr(VI) ion by Pd-Fe/NMC from high chromium state to lower oxidation chromium (Dandapat et al. 2011). The catalytic reduction of Cr(VI) was a reliably effective method.

It is demonstrated that the temperature had a greater influence on the catalytic reduction of chromium, while the surface acidities of catalysts increased with temperature increasing from 85.9 to 96.6 % and 99.9 %, respectively. The optimal temperature catalytic reduction of Cr(VI) was at 30 °C.

Catalytic activity and control study

As is shown in Fig. 9, it is demonstrated that dichromate reduction was used to assess the catalytic activity and simple in situ reaction of Pd-Fe/NMC catalysts. For this, iron and nitrogen-functionalized mesoporous carbon (Fe/NMC) were populated with Pd nanoparticles via $PdCl_2$ precursor. After adding sodium formate reducing agent, these Pd-Fe/NMC catalysts were infused into mixture solution to catalyze chromate reduction by measuring the absorbance of the solution to determine the reduction of chromium via UV/vis spectrophotometer.

First, we used some of the negative control research to check and confirm the performance of Pd-Fe/NMC catalysts. The conversion of 50 mg/L Cr(VI) to Cr(III) achieved as high as 99.97 % after 20 min when Pd-Fe/NMC catalysts were added, shown in Fig. 9. It was observed that 88 % of total Cr(VI) was decreased within the first 10 min. The HCOONa-induced Cr(VI) reduction rate without Pd-Fe/NMC catalysts was much slower than the reduction speed with Pd-Fe/NMC composite material. The chromium removal efficiency only realized 35 % until the end of the 20-min period. This apparent

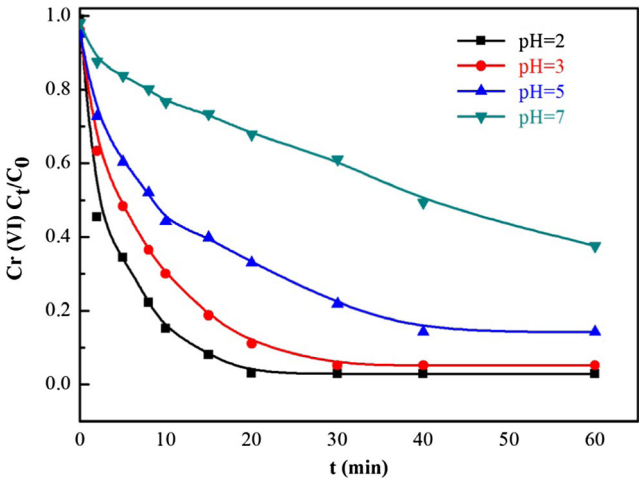

Fig. 7 Effect of pH values on reduction of Cr(VI) by Pd/Fe-NMC at 30 °C (initial Cr(VI) concentration 50 mg/L, HCOONa concentration 600 mg/L, Pd-Fe/NMC dosage 8 mg)

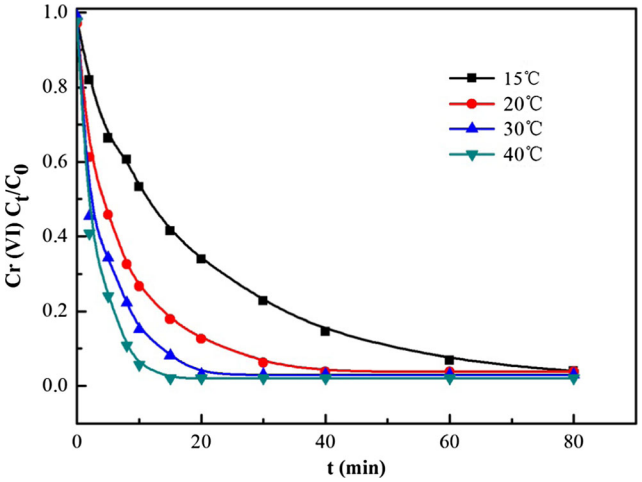

Fig. 8 Effect of temperature on reduction of Cr(VI) by Pd/Fe-NMC (initial Cr(VI) concentration 50 mg/L, HCOONa concentration 600 mg/L, Pd-Fe/NMC dosage 8 mg, pH 2.0)

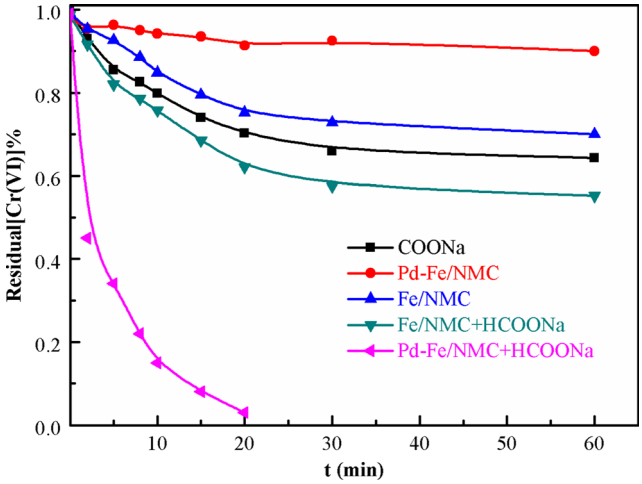

Fig. 9 Effect of catalytic activity and control study on reduction of Cr(VI) at 30 °C (initial Cr(VI) concentration 50 mg/L, HCOONa concentration 600 mg/L, Pd-Fe/NMC dosage 8 mg, pH 2.0)

declining difference in catalytic activity between Pd-Fe/NMC and Fe/NMC catalysts may be because of the specific surface area shown in images of Fig. 4. It is also shown that the reduction efficiency of NMC and Fe/NMC composite is significantly lower than that with load of Pd-Fe/NMC and leads to much less catalytic reduction activity, even no catalytic activity with the passage of time.

As a result, it was difficult to reduce Cr(VI) to any degree in water by Fe/NMC. Therefore, we can draw a conclusion that the Pd-Fe/NMC has advantages in Cr(VI) catalytic reduction reaction from obvious priority in the conversion. To quantitatively research and confirm the mechanism, the linear regression analysis was used to the conduct relationship between reaction time and Ln(C_t/C_0). The removal slopes of aqueous Cr(VI) obtained from these linear regressions were well followed with pseudo-first-order kinetic model, where the observed rate is proportional to the aqueous Cr(VI) concentration.

$$-K_{obs}[\mathrm{Cr(VI)}] = d_{[\mathrm{Cr(VI)}]}/d_t \quad (4)$$

where [Cr(VI)] is the concentration of aqueous Cr(VI), t is the time, and K_{obs} is the observed pseudo-first-order rate constant. The calculation of linear regression of ln[Cr(VI)] vs time (min) provided comparative Cr(VI) removal rates between the experiments with the corresponding initial concentration of Cr(VI). The Cr(VI) removal data in the whole experiment process was applied in the calculation, where active Cr(VI) removal took place (Yang et al. 2010). When the formate concentration was high, the concentration of formate could be regarded as constant in the whole experiment reaction process, and the dichromate reduction reaction conformed to the pseudo-first-order kinetics model in theory (Jeen et al. 2008).

It was notable that the Pd-Fe/NMC had the highest rate constant, 0.1625 min^{-1}, while Fe/NMC showed only 0.0493 min^{-1}, and HCOONa had only 0.070 min^{-1}. Fe/NMC and Pd-Fe/NMC also showed low rate constants, only 0.0313 min^{-1} and 0.017 min^{-1}, respectively. Both the rate constant and the conversion curve comparison analysis completely suggested the catalytic activity and the advantages of the proposed approach utilized for Pd nanocatalyst synthesis.

Effect of sodium formate concentration

Next, it is shown in Fig. 10 that the reaction rate was affected by different concentrations of sodium formate (HCOONa) which acted as the electron donor, using a fixed Pd-Fe/NMC NPs loading of 0.8 mg/mL at a fixed temperature (30 °C). The experiment showed that the catalytic reduction reaction needs the high concentration of reducing agent. The removal rate of Cr(VI) was only 40 % in 20 min with 150 mg/L sodium formate. However, the conversion of Cr(VI) came up to 97 and 100 % with 600 and 1000 mg/L sodium formate (Bhowmik et al. 2014). It was demonstrated that the proper reducing agent has a great role on the catalytic reduction of chromium.

Effect of Cr(VI) concentration and the dosage of Pd-Fe/NMC

Figure 11 reflects that the catalytic reduction of chromium was influenced by the initial Cr(VI) concentration. The best concentration was at 50 mg/L where the chromium was completely reduced within 30 min. Moreover, the increasing initial Cr(VI) concentration resulted in initial catalytic reduction rate decreasing dramatically. The removal rates of Cr(VI) reached 100, 97, 73, and 54 % at initial concentrations of 50, 80, 120, and 200 mg/L, respectively. The reduction catalytic activities of Pd-Fe/NMC

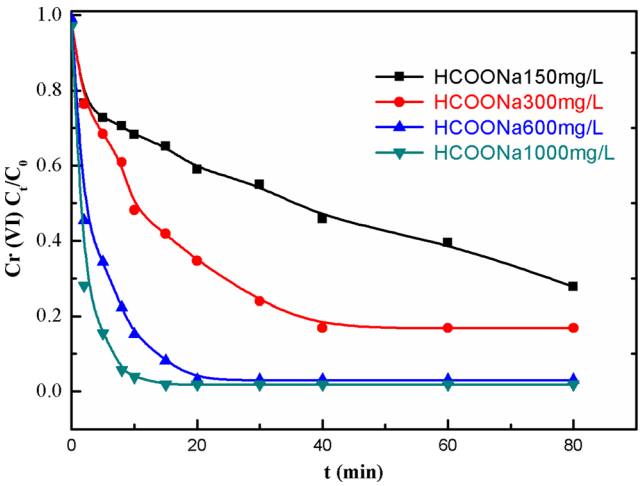

Fig. 10 Effect of sodium formate concentration on reduction of Cr(VI) by Pd/Fe-NMC at 30 °C (initial Cr(VI) concentration 50 mg/L, Pd-Fe/NMC dosage 8 mg, pH 2.0)

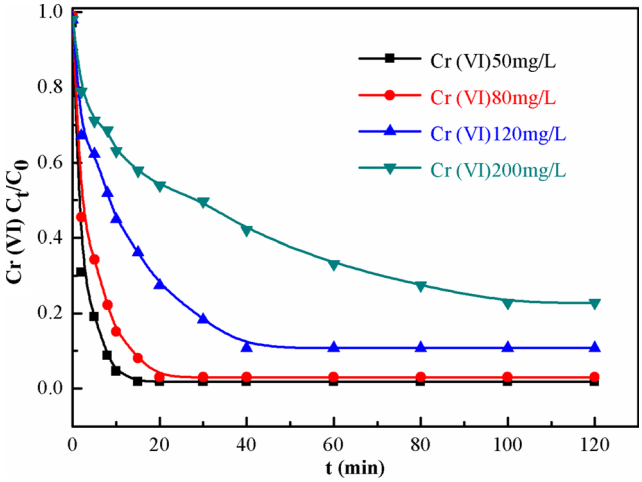

Fig. 11 Effect of Cr(VI) concentration on reduction of Cr(VI) by Pd/Fe-NMC at 30 °C (initial HCOONa concentration 600 mg/L, Pd-Fe/NMC dosage 8 mg, pH 2.0)

decreased with the increase of initial concentration, which could be due to surface active sites blocked by Cr(VI) (Fig. 11) (Huang et al. 2012). The plot and linear regression of ln [Cr(VI)] vs. time at different initial Cr(VI) concentrations are shown Fig. 12, and the pseudo-first-order reaction rate constant was calculated (shown in Table 2). The reduction only conforms to pseudo-first-order kinetics at low initial concentration rather than higher initial concentrations, which is consistent with previous literature (Gehringer and Eschweiler 2002). This is caused by a lack of HCOONa to reduce high concentrations of chromium (VI) (Tang et al. 2016).

As is shown in Fig. 13, the surface reduction activity of chromium (VI) increased with increasing the concentration of

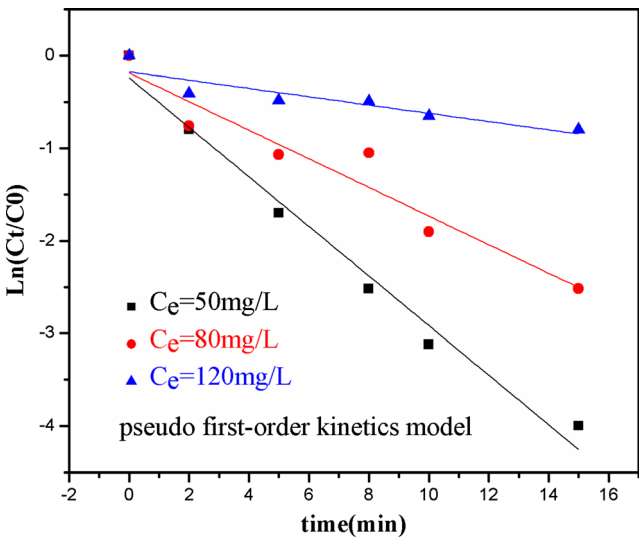

Fig. 12 Plot of ln [Cr(VI)] vs. time under different initial Cr(VI) concentrations at 30 °C (HCOONa concentration 600 mg/L, Pd-Fe/NMC dosage 8 mg, pH 2.0)

Table 2 k_{app} values with respect to the concentration of Cr(VI)

C_e (mg)	k_{app}
50	0.267
80	0.154
120	0.044

palladium catalyst significantly, indicating that the concentration of reactive species was dependent on Pd-Fe/NMC dosage.

Regeneration of Pd-Fe/NMC

Considering the reaction conditions during the acidity may have effect on the Pd stabilization of the mesoporous composites, it is nonetheless worth conducting regeneration experiments to investigate the stability and reusability of Pd-Fe/NMC catalyst. For this, thoroughly rinsed Pd-Fe/NMC was directly used for the next reaction cycle with ultrapure water washing to neutral after each batch reaction. As seen in five consecutive cycles (Fig. 14), the reduction efficiencies decreased less than 5 % of the initial activity after a cycle and preserved at a high level with above 75 % for Cr(VI) removal in the fifth cycle, suggesting that Pd was fixed in the Fe/NMC mesoporous composites fairly steadily (Andrzej et al. 2000).

Result showed that it was similar to the reduction of Cr(VI) with amino-functionalized palladium nanowires as for the regeneration and reuse performance of Pd-Fe/NMC (Tang et al. 2015) and Pd nanoparticles supported mesoporous γ-Al_2O_3 film for reduction of Cr(VI) using formic acid reported (Dandapat et al. 2011) in previous studies, showing the super reduction efficiency of the mesoporous particle. Hence, we can conclude that the Pd-Fe/NMC might provide an effective catalytic

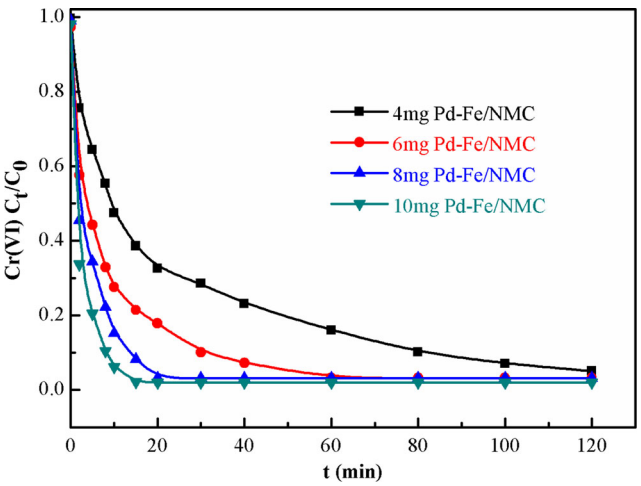

Fig. 13 Effect of the dosage of Pd-Fe/NMC on reduction of Cr(VI) by Pd/Fe-NMC at 30 °C (initial Cr(VI) concentration 50 mg/L, initial HCOONa concentration 600 mg/L, pH 2.0)

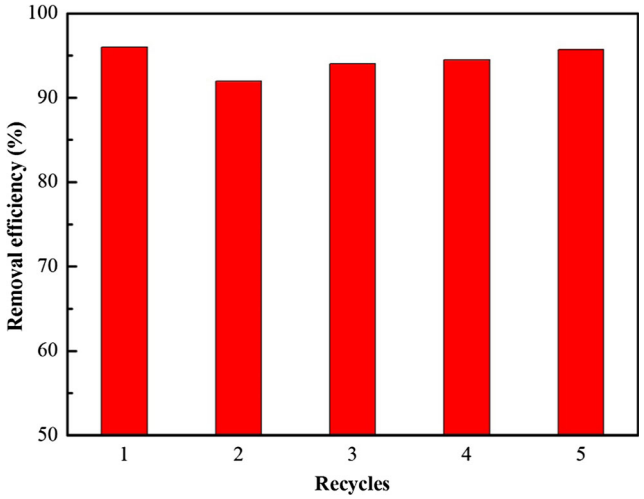

Fig. 14 Regeneration of Pd-Fe/NMC on reduction of Cr(VI) by Pd/Fe-NMC at 30 °C (initial Cr(VI) concentration 50 mg/L, initial HCOONa concentration 600 mg/L, Pd-Fe/NMC dosage 8 mg, pH 2.0)

treatment to reduce the heavy metals because of the magnetic separation and outstanding ability in water environment treatment by in situ regeneration and reuse.

Conclusion

In this work, it is convinced that the stability and reusability of the Pd/Fe-NMC catalysts were excellent and the catalytic activity of Pd/Fe-NMC was sustainable to reduce Cr(VI). The pH of solution and the electron donor sodium formate (HCOONa) affected the catalytic reduction activities obviously. It was found that the optimal pH to remove chromium value was at 2 with 600 mg/L HCOONa. The dichromate reduction reaction conformed to the pseudo-first-order kinetics model. It is shown that the reduction catalytic activities of Pd-Fe/NMC declined as the initial concentration increased in the research, and the most suitable initial concentration was at 50 mg/mL which completed the reduction within 30 min. The materials could be regenerated by 0.01 M NaOH and reused, which indicated that the Pd-Fe/NMC was cost-effective. All in all, we can make a conclusion that the Fe-NMC composite owned the high surface area as the carrier of palladium catalyst and can potentially promote the catalytic reduction of chromium (VI) in water treatment.

Acknowledgments The study was financially supported by the National Program for Support of Top–Notch Young Professionals of China (2012), Projects 51579096, 51222805, 51521006, and 51508175 supported by the National Natural Science Foundation of China, the Program for New Century Excellent Talents in University from the Ministry of Education of China (NCET–11–0129), the Hunan Province Innovation Foundation for Postgraduate (CX2015B095).

References

Andrzej B, Andrzej C (2000) The kinetic model of hydrogenation of acetylene–ethylene mixtures over palladium surface covered by carbonaceous deposits. Appl Catal A-Gen 198:51–56

Basu A, Johnson TM (2012) Determination of hexavalent chromium reduction using Cr stable isotopes: isotopic fraction factors for permeable reactive barrier materials. Environ Sci Technol 46:5353–5360

Bhowmik K, Mukherjee A, Mishra M, De G (2014) Stable Ni nanoparticle − reduced graphene oxide composites for the reduction of highly toxic aqueous Cr(VI) at room temperature. Langmuir 30:3209–3216

Chaplin BP, Reinhard M, Schneider WF, Schueth C, Shapley JR, Strathmann T, Werth CJ (2012) A critical review of Pd-based catalytic treatment of priority contaminants in water. Environ Sci Technol 46:3655–3670

Chen H, Shao Y, Xu ZY, Wan HQ, Wan YQ, Zheng SR, Zhu DQ (2011a) Effective catalytic reduction of Cr(VI) over TiO_2 nanotube supported Pd catalysts. Appl Catal B-Environ 105:255–262

Chen T, Wang T, Wang DJ, Xue H-R, Zhao JQ, He JP (2011b) Synthesis of ordered large-pore mesoporous carbon for Cr(VI) adsorption. Mater Res Bull 46:1424–1430

Chi Y, Geng WC, Zhao L, Yan X, Yuan Q, Li N, Li XT (2012) Comprehensive study of mesoporous carbon functionalized with carboxylate groups and magnetic nanoparticles as a promising adsorbent. J Colloid Interface Sci 369:366–372

Dandapat A, Jana D, De G (2011) Pd nanoparticles supported mesoporous $\gamma - Al_2O_3$ film as a reusable catalyst for reduction of toxic Cr(VI) to Cr (III) in aqueous solution. Appl Catal A-Gen 396:34–39

Donmez G, Aksu Z (2002) Removal of chromium (VI) from saline wastewaters by Dunaliella species. Process Biochem 38:751–762

Elliott DW, Zhang WX (2001) Field assessment of nanoscalebiometallic particles for groundwater treatment. Environ Sci Technol 35:4922–4926

Fathi D (2012) Radiolytic formation of non-toxic Cr(III) from toxic Cr(VI) in formate containing aqueous solutions: a system for water treatment. J Hazard Mater 223–224:104–109

Fruchter J (2002) In situ treatment of chromium-contaminated groundwater. Environ Sci Technol 36(A):464–472

Gao Y, Xia J (2011) Chromium contamination accident in China: viewing environment policy of China. Environ Sci Technol 45:8605–8606

Gehringer P, Eschweiler H (2002) The dose rate effect with radiation processing of water an interpretative approach. Radiat Phys Chem 65:379–386

Hu C, Ting SW, Chan KY, Huang W, Int J (2012) Reaction pathways derived from DFT for understanding catalytic decomposition of formic acid into hydrogen on noble metals. Int J Hydrog Energy 37:15956–15965

Huang YP, Ma H, Wang SG, Shen MW, Guo R, Cao XY, Zhu MF, Shi XY (2012) Efficient catalytic reduction of hexavalent chromium using palladium nanoparticle-immobilized electrospun polymer nanofibers. ACS Appl Mater Interfaces 4:3054–3061

Jeen SW, Blowes DW, Gillham RW (2008) Performance evaluation of granular iron for removing hexavalent chromium under different geochemical conditions. J Contam Hydrol 95:76–91

Jin Y, Lee SY (2014) Use of tyrosyl bolaamphiphile self-assembly as a biochemically reactive support for the creation of palladium. ACS Appl Mater Interfaces 6:6461–6468

Kim SD, Park KS, Gu MB (2002) Toxicity of hexavalent chromium to *Daphnia magna*: influence of reduction reaction by ferrous iron. J Hazard Mater 93:155–164

Krishnani KK, Srinives S, Mohapatra BC, Boddu VM, Hao J, Meng X, Mulchandani A (2013) Hexavalent chromium removal mechanism using conducting polymers. J Hazard Mater 99-106:252–253

Liang M, Su RX, Qi W, Zhang Y, Huang RL, Yu YJ, Wang LB, He Z (2014) Reduction of hexavalent chromium using recyclable Pt/Pd nanoparticles immobilized on procyanidin-grafted eggshell membrane. Ind Eng Chem Res 5313:635–13643

Liu NN, Yin LW, Wang CX, Zhang LY, Lun N, Xiang D, Qi YX, Gao R (2010) Adjusting the texture and nitrogen content of ordered mesoporous nitrogen doped carbon materials prepared using SBA-15 silica as a template. Carbon 48:3579–3591

Ludwig R, Su CM, Lee TR, Wilkin RT, Acree SD, Ross RR, Keeley A (2007) In situ chemical reduction of Cr(VI) in groundwater using a combination of ferrous sulfate and sodium dithionite. Environ Sci Technol 41:5299–5305

Mertz W (1969) Chromium occurrence and function in biological systems. Phys Rev 49:163–239

Omole MA, K'Owino IO, Sadik OA (2007) Palladium nanoparticles for catalytic reduction of Cr(VI) using formic acid. Appl Catal B-Environ 76:158–167

Pang Y, Zeng GM, Tang L, Lei XX, Li Z, Zhang C, Xie GX (2011a) PEI-grafted magnetic porous powder for highly effective adsorption of heavy metal ions. Desalination 281:278–284

Pang Y, Zeng GM, Tang L, Zhang Y, Liu YY, Lei XX (2011b) Preparation and application of stability enhanced magnetic nanoparticles for rapid removal of Cr(VI). Chem Eng J 175:222–227

Qian A, Liao P, Yuan SH, Luo MS (2014) Efficient reduction of Cr(VI) in groundwater by a hybrid electro-Pd process. Water Res 48:326–334

Shevchenko N, Zaitsev V, Walcarius A (2008) Bifunctionalized mesoporous silicas for Cr(VI) reduction and concomitant Cr(III) immobilization. Environ Sci Technol 42:6922–6928

Shrestha SJ, Asheghi SS, Timbro J, EMustain WE (2013) Effects of pore structure in nitrogen functionalized mesoporous carbon on oxygen reduction reaction activity of platinum nanoparticles. Carbon 60:28–40

Tang L, Yang GD, Zeng GM, Cai Y, Li SS, Zhou YY, Pang Y, Liu YY, Zhang Y, Luna B (2014) Synergistic effect of iron doped ordered mesoporous carbon on adsorption-coupled reduction of hexavalent chromium and the relative mechanism study. Chem Eng J 239:114–112

Tang L, Tang J, Zeng GM, Yang GD, Xie X, Zhou YY, Pang Y, Fang Y, Wang JJ, Xiong WP (2015) Rapid reductive degradation of aqueous p-nitrophenol using nanoscale zero-valent iron particles immobilized on mesoporous silica with enhanced antioxidation effect. Appl Surf Sci 333:220–228

Tang L, Xie ZH, Zeng GM, Dong HR, Fan CZ, Zhou YY, Wang JJ, Deng YC, Wang JJ, Wei X (2016) Removal of bisphenol a by iron nanoparticle-doped magnetic ordered mesoporous carbon. RSC Adv 25(6):724–25732

Wang P, Lo IMC (2009) Synthesis of mesoporous magnetic-Fe_2O_3 and its application to Cr(VI) removal from contaminated water. Water Res 43:3727–3734

Wang ZL, Liu XJ, Lv MF, Meng J (2010) Simple synthesis of magnetic mesoporous FeNi/carbon composites with a large capacity for the immobilization of biomolecules. Carbon 48:3182–3189

Wattsa MP, Coker VS, Parry SA, Thomas RAP, Kalin R, Lioyed JR (2015) Effective treatment of alkaline Cr(VI) contaminated leachate using anovel Pd-bionanocatalyst: impact of electron donor andaqueous geochemistry. Appl Catal B-Environ 170-171:162–117

Wei LL, Gu R, Lee JM (2015) Highly efficient reduction of hexavalent chromium on amino-functionalized palladium nanowires. Appl Catal B-Environ 17:6325–6330

Yang CX, Manocchi AK, Lee B, Yi H (2010) Viral templated palladium nanocatalysts for dichromate reduction. Appl Catal B-Environ 93: 282–291

Yang C, Meldon B, Lee B, Yi H (2014) Investigation on the catalytic reduction kinetics of hexavalent chromium by viral-templated palladium nanocatalysts. Catal Today 233:108–116

Zhao DY, Huo QS, Feng JL, Chmelka BF, Stucky GD (1998) Nonionic triblock and star diblock copolymer and oligomeric surfactant syntheses of highly ordered, hydrothermally stable mesoporous silica structures. J Am Chem Soc 120(24):6024–6036

Zhou XJ, Korenaga T, Takahashi T, Moriwake T, Shinoda S (1993) A process monitoring controlling system for the treatment of wastewater containing chromium (VI). Water Res 27:1049–1054

Zhou YY, Tang L, Yang GD, Zeng GM, Deng YC, Huang BB, Cai Y, Tang J, Wang JJ, Wu YN (2016) Phosphorus-doped ordered mesoporous carbons embedded with Pd/Fe bimetal nanoparticles for the dechlorination of 2,4-dichlorophenol. Catal Sci & Technol 6:1930–1939